



Dissolution behavior and kinetic investigation of Ca²⁺ in the dissolution of colemanite in propionic acid presence saturated with synthetic flue gas

Mücahit Uğur ^{1,*}

¹Çankırı Karatekin University, Faculty of Engineering, Department of Chemical Engineering, Çankırı,18100, Türkiye

ARTICLE INFO

Article history:

Received October 25, 2023

Accepted January 21, 2024

Available online March 29, 2024

Research Article

DOI: 10.30728/boron.1380919

Keywords:

Colemanite

Dissolution kinetics

Heterogeneous reaction

Propionic acid

Synthetic flue gas

ABSTRACT

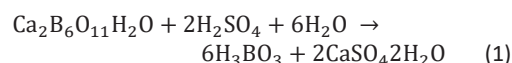
Colemanite $2\text{CaO} \cdot 3\text{B}_2\text{O}_3 \cdot 5\text{H}_2\text{O}$ is a calcium borate mineral and can be expressed as the basic material of industrial boric acid production. Boric acid is one of the most important raw materials obtained by dissolving colemanite ore in acidic solutions or gases. This study aims to determine an alternative reactant for boric acid production by examining the dissolution behavior and kinetics of Ca²⁺ passing into solution in propionic acid solution saturated with synthetic flue gas of colemanite. For the first time in this study, colemanite ore was dissolved simultaneously in a gas and acid environment. The use of this acid and gas as a solvent is an alternative reactant due to the current process and less occurrence of impurities originating from colemanite. In this context, the effects of reaction temperature, solid-liquid ratio, grain size, acid concentration, and synthetic flue gas flow rate parameters were investigated. According to experimental data, the amount of Ca²⁺ passing into the solution has been observed that the reaction temperature, acid concentration, and gas flow rate increase and the solid-liquid ratio and grain size decrease. Experimental data were successfully correlated with linear regression using the Statistica package program and analyzed according to homogeneous and heterogeneous reaction rate models. It is seen that the dissolution of Ca²⁺ passing into the solution fits the "Avrami model" and the activation energy $26.83 \text{ kJ} \cdot \text{mol}^{-1}$ value also confirms this model.

1. Introduction

Boron and boron compounds are some of the most important minerals in the world in terms of industrial and technological applications. Boron reserves are widely found in Türkiye, Russia, USA, and China. Türkiye has approximately 72% of the world's boron reserves [1]. Boron based minerals are undoubtedly one of the most important underground ore of Türkiye in terms of reserve amount and diversity [2]. Thanks to these superiorities, boron minerals are important in obtaining technological products and materials, contributing to the production of environmentally friendly and innovative technologies [3]. Although there are more than 200 boron compounds in nature, only a few of them have the opportunity to be used commercially and industrially [4]. In terms of the amount of reserves in Türkiye, tincal ($\text{Na}_2\text{O}_2 \cdot \text{B}_2\text{O}_3 \cdot 10\text{H}_2\text{O}$), colemanite ($\text{Ca}_2\text{B}_6\text{O}_{11} \cdot 5\text{H}_2\text{O}$) and ulexite ($\text{Na}_2\text{O}_2 \cdot \text{CaO}_5 \cdot \text{B}_2\text{O}_3 \cdot 16\text{H}_2\text{O}$) minerals are widely found [5-7]. Although boron is a nonmetal in group IIIA, it sometimes shows metallic properties [8]. Its different properties displayed in its compounds with various metal or nonmetallic elements allow the use of many boron compounds in industry. These minerals are used in different applications in the fiberglass [9], metallurgy, energy storage, defense

industry, waste disposal [10,11], nuclear applications and catalysts, polymer industry [12], rubber, paint, and textile industries [13]. In Türkiye, boric acid production in industry consists of reaction of sulphuric acid with colemanite [14].

As seen in Eq. (1), borogypsum is formed as a by-product besides boric acid.



Kurtbaş et al. dissolved the colemanite in a solution of boric acid saturated with SO₂ gas, which is used as an alternative solvent. The reaction was found to be compatible with the first-order homogeneous model and the E was found to be $50.15 \text{ kJ} \cdot \text{mol}^{-1}$ [15]. Guliyev et al. examined the dissolution kinetics of colemanite in ammonium hydrogen sulfate presence and tried to determine an alternative solvent for boric acid production. It was determined that the diffusion control from the product film with an activation energy of $32.66 \text{ kJ} \cdot \text{mol}^{-1}$ fits the model [16]. Kızılcıca and Çopur dissolved the colemanite in the presence of methanol in the pressurized reactor environment and determined that it followed the second-order homogeneous model with

*Corresponding author: m.ugur@karatekin.edu.tr

an activation energy of 51.4 kJ.mol^{-1} [17]. In the study of Karagöz and Kuşlu, colemanite ore was dissolved with potassium dihydrogen sulfate. The suitability of the process to the chemical reaction-controlled model was determined and the activation energy was found to be $41.88 \text{ kJ.mol}^{-1}$ [18]. Mumcu et al. provided dissolution of colemanite ore in sodium bisulfate solution as an alternative solvent. In a two-stage dissolution process; the dissolution rate was defined from with diffusion-controlled model from ash film with activation energies of 3.4 kJ.mol^{-1} and 6.1 kJ.mol^{-1} , respectively [14]. Sis et al. investigated the dissolution of colemanite in an aqueous medium in the presence of hydrochloric acid and it was determined that the reaction rate conformed to the Avrami model [19].

In Türkiye, an average of 385 thousand tons/year of boric acid is produced from the reaction of colemanite with H_2SO_4 , while 855-1155 thousand tons/year of borogypsum is produced two to three times this amount [8]. Since the B_2O_3 contained in the structure of borogypsum will dissolve with rainwater, it mixes with soil and water and causes environmental pollution [20]. H_2SO_4 , a strong acid used in the industrial process, provides the dissolution of limestone, dolomite containing Ca^{2+} and Mg^{2+} in colemanite structures, and clay structures containing Mg^{2+} . When these minerals react with sulfuric acid, which is a strong acid, or dissolve with boric acid, a significant amount of ions pass into the solution, which will reduce the efficiency of the process [21]. The only source of these impurities is not the clays in the structure, but also the SO_4^{2-} impurity coming from sulfuric acid.

This must be carried out in an environment that will not affect the side minerals or will affect them only slightly, to eliminate the situations that will cause environmental pollution and the impurities coming from the colemanite structure and H_2SO_4 [22]. Acetic acid, propionic acid, and similar acids with longer carbon chains can be used for this purpose [23]. Studies on this subject have shown that impurities passing into solution in reactions carried out with organic acids can be controlled [23]. In this study, to minimize the problem of impurities in boric acid production, we reduced the dissolution of side minerals in the ore and used propionic acid as a solvent together with synthetic flue gas to determine the maximum dissolution conditions of the ore. It is more advantageous to use propionic acid because it has weaker acidic properties than H_2SO_4 and acetic acid and its boiling point is higher than acetic acid. Thus, the low amount of evaporated acid provides an advantage for the environment and health. Calcium propionate $\text{Ca}(\text{CH}_3\text{CH}_2\text{COO})_2$ is formed as a by-product in the production of boric acid from propionic acid and colemanite. Calcium propionate, which also has commercial value, is widely used both as a preservative additive in bakery and bread and in the food industry for protective bacteria and fungi [24]. In addition, while boric acid is produced from sulfuric acid, waste gypsum, which causes environmental pollution, is prevented from polluting nature. Dissolving

colemanite in a propionic acid solution saturated with synthetic flue gas produces purer boric acid and does not create an extra economical situation for removing impurities. In addition, instead of borogypsum, which creates environmental pollution, calcium sulfide ($\text{CaSO}_3 \cdot 0.5\text{H}_2\text{O}$), which has high added value, is formed. Sulfuric acid is generally used in known methods of producing boric acid. Gases such as CO_2 or SO_2 are also used in the literature. Compared to the usual methods using sulfuric acid, in the process will require additional investment costs. For the first time in this study, colemanite ore was dissolved simultaneously in a gas and acid environment. The use of this acid and gas as a solvent is an alternative reactant due to the current process and less occurrence of impurities originating from colemanite. On the other hand, it is thought that the properties of the boric acid obtained will be purer in terms of sulfate, calcium, and magnesium. There is no study in the literature on the simultaneous dissolution of colemanite in both gas and acidic solution environments. For this reason, the investigation of the dissolution effect in propionic acid solutions saturated with synthetic flue gas is of great importance in terms of literature.

There is no study in the literature on the simultaneous dissolution of colemanite in both gas and acidic solution environments. For this reason, the investigation of the dissolution effect in propionic acid solutions saturated with synthetic flue gas is of great importance in terms of literature. In addition, a new reactant for boric acid production will be determined.

2. Material and Methods

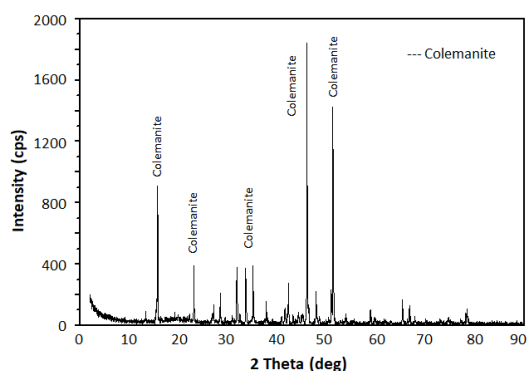
2.1. Material

The colemanite ore used in the experimental procedure was obtained from the Emet Boric Acid Factory of Eti Mine Works. Visible impurities on the mineral were cleaned and ground with a grinder in a laboratory environment. Sieves in different size ranges in ASTM E-11 standards are divided into fractions of 100-150, 150-250, 250-400, and 400-600 μm with a Restch A-5200 brand vibrating sieve device. In the kinetic calculations, the arithmetic average of these particle sizes was used. The moisture in the ore was completely removed by keeping the experiment samples in an oven at 100°C until the mass change ceased. The propionic acid of 99% purity used in the study was obtained from Merck and synthetic flue gas (13% SO_2 , 7% O_2 , and 80% N_2) was obtained from Ankara gas companies. Chemical analysis of colemanite was determined by atomic absorption spectrophotometric and titrimetric gravimetric methods, and the results are given in Table 1. According to the table, the ore used contains 34.21% B_2O_3 and 19.24% CaO , and this value indicates that the ore used contains 67.12% colemanite. Also, the CaO percentage coming from colemanite is 9.3% and the CaO percentage coming from non-colemanite sources is 9.94. The latter is found in the form of calcite in ore.

Table 1. The chemical composition of colemanite.

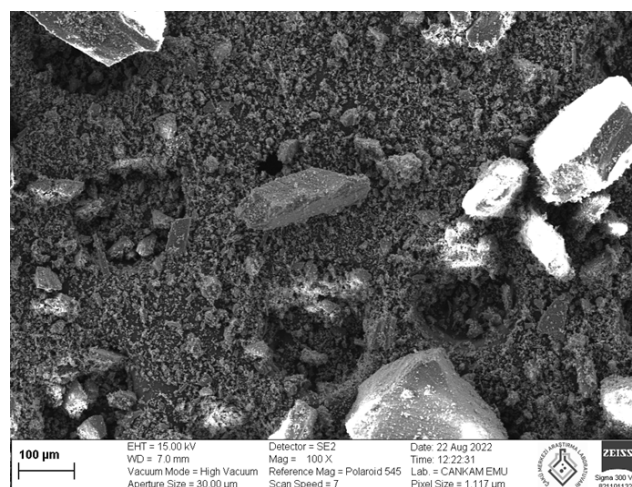
Component	B ₂ O ₃	CaO	H ₂ O	MgO	Moisture	Others
%	34.21	19.24	14.66	1.72	0.71	29.46

Measurements were made with the Bruker brand D8 Discover model, which is based on the X-Ray diffraction method (XRD), which is based on the principle that each crystalline phase refracts X-Rays in a characteristic pattern depending on its unique atomic arrangements. SEM is a type of electron microscope that obtains images by scanning the sample surface with a focused electron beam. Analyzes were carried out with the Carl Zeiss brand Sigma 300 VP model, which works according to the logic that electrons interact with the atoms in the sample and produce different signals containing information about the topography and composition of the sample surface. XRD and SEM analyses of the structural analysis of the colemanite ore were performed and are given in Figure 1 and Figure 2.

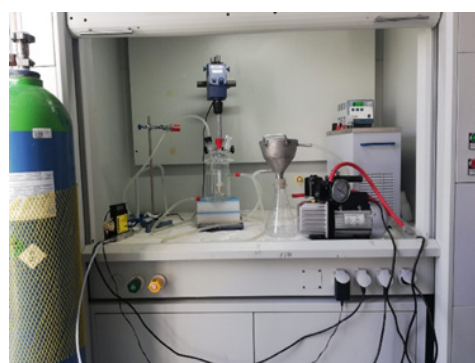
**Figure 1.** XRD analysis of colemanite ore.

2.2. Methods

The parameters and levels of the kinetic study experiments were determined considering the preliminary test results and literature information. The theoretical acid amount and excess acid concentrations that should be consumed in the dissolution reaction of colemanite and propionic acid were determined. Fixed parameters indicated with a symbol of (*) in Table 2 were used to determine the effect of a parameter more clearly in dissolution experiments. The particle size is given in Table 2. in the form of two size ranges and the arithmetic mean value of these two dimensions is used in kinetic calculations. The experimental plan and number of the study are given in Appendix 1.

**Figure 2.** SEM image of colemanite ore.

In this study, experiments were carried out under atmospheric pressure and in a double-walled 500 mL glass reactor. Polyscience SD20R-30-A12E brand temperature circulator was used to keep the solution in the reactor at a certain and constant temperature during leaching. Mechanical mixer with Scilogex OS20-Pro brand tachometer with digital display for homogenization of the solution and mixing, Aalborg brand GFC17 model digital flow meter for sending synthetic flue gas to the reactor at a certain flow rate, and Value VE-225SV brand vacuum pump was used in the filtration stage of the experimental solutions. The experimental system used during solving in the laboratory is given in Figure 3.

**Figure 3.** The system used in the experimental studies.**Table 2.** The parameters and levels used in the experiment.

Parameters	Levels
A Reaction Temperature (K)	283,293, 303* ,313,323
B Solid/Fluid Ratio (g/L)	20, 40* ,60,80
C Particle Size (μm)	100-150,150-250, 250-400* ,400-600
D PA Concentration (M)	0,0.3375, 0.675 ,1.335
E SFG Flow Rate (L/min)	0.05, 0.10* ,0.15

*Parameter that remains constant while examining the effect of another parameter.

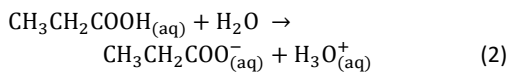
In the dissolution process, propionic acid/water at the desired rate is taken into a 500 mL double-walled glass reactor, and then it reaches the desired temperature. The solution, which reached a specific temperature, was saturated with synthetic flue gas containing SO₂ and then the dissolution reaction was started by adding colemanite ore. Solutions in the form of suspensions were taken and filtered at certain times within 60 minutes, which was determined as the total dissolution time. At the end of the experiment, the entire suspension solution was filtered and the solid residue was dried at ambient temperature.

The radiation emitted from the hollow cathode lamp used specifically for the measured element was passed through the existing flame measured by a segmented solid-state detector and analyzed with a Shimadzu AA-7000 model Atomic Absorption Spectrophotometer. The amount of in the experiment samples taken was determined with an Atomic Absorption Spectrophotometer and was stated as the percent solution passing rate in the calculations. Fourier Transform Infrared Spectrophotometry (FTIR) analysis was performed to determine the structure of the solid residue formed due to the experimental study and the presence of functional groups. Measurements were made with the Bruker Tensor II Diamond ATR-FTIR device, which has a resolution of 4 cm⁻¹ and a wavelength between 400 and 4000 cm⁻¹. Kinetic modeling data were determined from percentage solution passing values with the help of the Statistica 10 package. In Eq.(16), the exponential constants (a, b, c, d, m) and the regression coefficient (r²) in the kinetic model were calculated statistically using the Statistica 10 package program, and the Arrhenius constant (A) and the activation energy (E) were calculated using the Arrhenius graph.

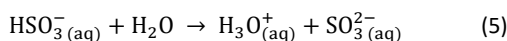
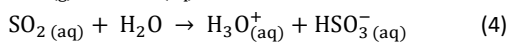
3. Results and Discussion

3.1. Reactions

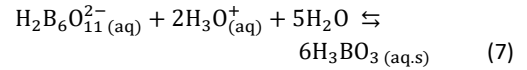
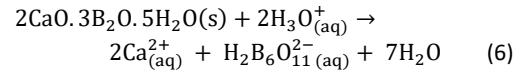
The ionization reaction of propionic acid in an aqueous solution can be written as:



Decomposition reactions of synthetic flue gas into ions in aqueous medium are as follows.

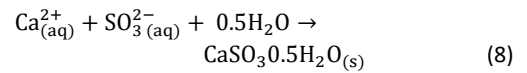


In addition to the reaction in Eq.(2), H₃O⁺ ions formed in Eq.(4) and (5) reactions dissolve the colemanite ore and form boric acid according to the following reactions.

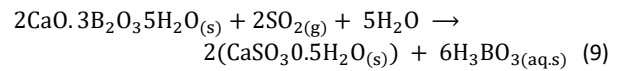


Due to Eq.(6) and Eq.(7) H₃O⁺ ions surrounding the particle decrease, and the acidity value of the solution increases. Eq.(8) shifts to the right and the SO₃²⁻ concentration increases.

When Ca²⁺ and SO₃²⁻ ions in the solution reach sufficient concentrations to ensure [Ca²⁺][SO₃²⁻][H₂O]^{0.5} > K_{sp}, calcium sulfite half mol aqueous CaSO₃·0.5H₂O(s), known as hannebachite, is formed.



The total reaction is given below Eq.(9):



Thus, a layer consisting of solid boric acid formed according to reaction 7 and calcium sulfite (CaSO₃·0.5H₂O) formed according to reaction 8 will form around the unreacted core. CaSO₃·0.5H₂O is solid and insoluble in water, but solid boric acid is soluble in it. For this reason, at any moment, a tight solid boric acid + CaSO₃·0.5H₂O layer controlling the reaction rate will form around the unreacted core and this layer, there will be a porous layer of CaSO₃·0.5H₂O layer including does not affect the reaction rate. X-ray diffraction and FTIR results of the solid residue occurring during experimental studies, seen in Figure 4 (a) and (b) confirm this.

3.2. Effect of Parameters

The effects of particle size, reaction temperature, propionic acid concentration, solid/liquid ratio, and synthetic flue gas flow rate on Ca²⁺ passing into SO₂ saturated solution were investigated. The graphs of fractions of Ca²⁺ passing to solution versus time were determined using the parameters and levels indicated in Table 2. For the kinetic calculation, the dissolution fraction of Ca²⁺ in the solution was calculated according to the Eq.(10).

$$\text{Dissolution fraction } X_{\text{Ca}}^{2+} = \frac{\text{Amount of Ca}^{2+} \text{ in solution (mg)}}{\text{The amount Ca}^{2+} \text{ in original ore (mg)}} \quad (10)$$

3.2.1. Effect of reaction temperature

Temperature is one of the most essential factors for dissolution kinetics. The effect of reaction temperature on the passing of Ca²⁺ ions in the structure of colemanite into solution was investigated at 283, 293, 303, 313, and 323 K. The graph of the obtained

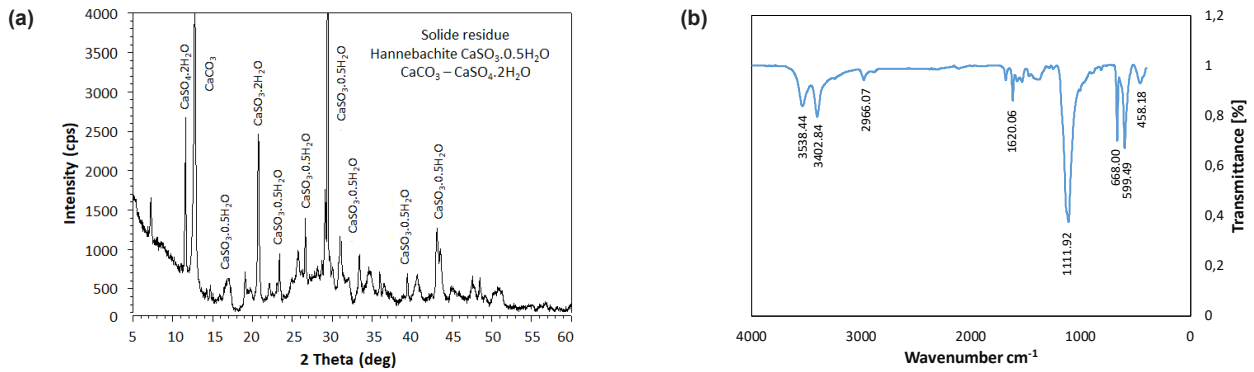


Figure 4. a) X-ray diffraction and b) FTIR results of the solid residue obtained in experiments.

dissolution percentages versus time is given in Figure 5. Since the kinetic energies of the molecules increase exponentially with the increase in temperature, it increases the collision rate of the molecules per unit of time [2,23,25,26]. For this reason, it is seen in Figure 5 that the increase in the reaction rate and the amount of Ca^{2+} passing into the solution in the aqueous medium with the increase in temperature.

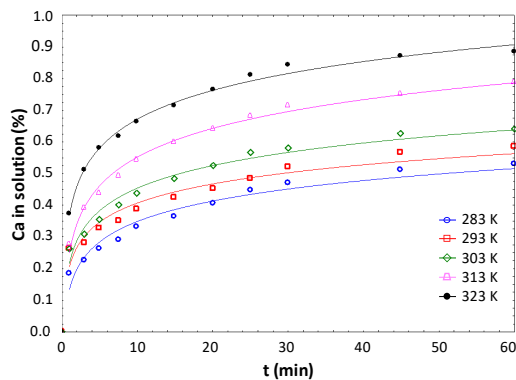


Figure 5. Effect of the reaction temperature on Ca^{2+} released during the dissolution of colemanite in SFG-saturated solution.

3.2.2. Effect of solid-liquid ratio

The effect of solid/liquid ratio on Ca^{2+} ions in the colemanite structure to passing into solution was investigated at 20, 40, 60, and 80 $g.L^{-1}$ ratios. The graph of the amount of Ca^{2+} ions passing into the solution versus time is shown in Figure 6. As shown in Figure 5 the increase in the solid/liquid ratio to causes a decrease in the dissolution rate of Ca^{2+} . This situation is due to the increase in the amount of reactant per unit solvent. Similar results were observed in the dissolution of colemanite ore in methanol, ammonium hydrogen sulfate, and sulfuric acid solutions [16,17,27]. On the other hand, the mass of Ca^{2+} ions passing to the solution under the same conditions increases as the solid/liquid ratio increases. As a matter of fact, at the end of the 60-minute experiments at 20, 40, 60 and 80 $g.L^{-1}$ solid/liquid ratios, the fractions of Ca^{2+} ions passing into the solution were 71.5, 64, 60 and 54%, respectively, while the mass values of Ca^{2+} ions passing into the solution were 982, 1605, 2142 and 3225 mg , respectively.

The physical values of the boric acid formed can be calculated or measured. For example, if 50% of colemanite is dissolved at a solid/liquid ratio of 20 $g.L^{-1}$, 10 g of colemanite will be used, 5 grams of which will be dissolved and 4.44 g of H_3BO_3 will be formed. Therefore, the boric acid concentration will be 4.44g/0.5 L = 8.88 $g.L^{-1}$. Since this is a low concentration, the calculable properties of boric acid and the yield of boric acid have not been calculated. Kinetic studies are performed at low solid/liquid ratios and only kinetics and reaction mechanisms are evaluated in these studies.

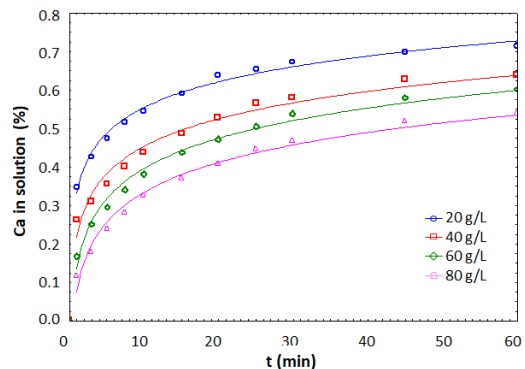


Figure 6. Effect of the solid/liquid ratio on Ca^{2+} released during the dissolution of colemanite in SFG saturated solution.

3.2.3. Effect of particle size

The effect of particle size on Ca^{2+} ions in the colemanite structure passes into solution was investigated using fractions of 100-150, 150-250, 250-400, and 400-600 μm . The graph of the passing values of Ca^{2+} ions into solution versus time is given in Figure 7. As seen in Figure 7, as the surface area of the amount of solid per solution amount increases with the increase in grain size, the amount of Ca^{2+} passing into the solution decreases. Therefore, it is expected that the decrease in particle size will increase the Ca^{2+} dissolution rate.

3.2.4. Effect of acid concentration

The effect of the propionic acid concentration on the rate of Ca^{2+} ions in the colemanite structure was examined at the concentrations of 0 M, 0.3375 M, 0.675 M, and

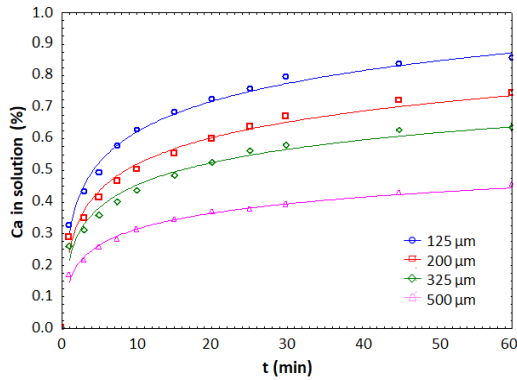


Figure 7. Effect of the particle size on Ca^{2+} released during the dissolution of colemanite in SFG saturated solution.

1.355 M. The graph of the passing values of Ca^{2+} ions to solution versus time is shown in Figure 8. As seen in Figure 8, the increase in propionic acid concentration increases the conversion rate of Ca^{2+} in the solution. This situation is thought to increase the hydronium ion (H_3O^+) in the solution with the increase of the propionic acid concentration and thus accelerate the reaction mechanism [12, 28]. According to Equation 9, the solid $\text{CaSO}_3 \cdot 0.5\text{H}_2\text{O}$ formed around the unreacted core has a more porous structure than the absence of propionic acid. For this reason, the dissolution reaction is expected to occur faster. If there is no propionic acid in the solution, the dissolution is carried out by the ions formed by the SO_2 in the SFG passed through the solution according to reactions 3-5. H_3O^+ ions dissolve the colemanite ore according to reactions 6 and 7. When Ca^{2+} and SO_3^{2-} ions in the solution reach sufficient concentration, hannebachite ($\text{CaSO}_3 \cdot 0.5\text{H}_2\text{O}$) is formed according to reaction 8. When propionic acid is added to the reaction medium, reactions 6-8 occur faster as the propionic acid concentration increases.

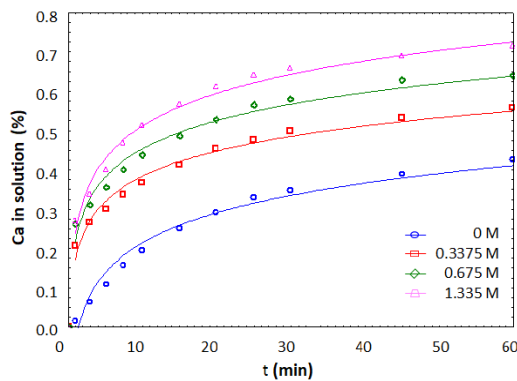


Figure 8. Effect of PA concentration on Ca^{2+} released during the dissolution of colemanite in SFG saturated solution.

3.2.5. Effect of synthetic flue gas

The effect of SFG on the rate of the passing of Ca^{2+} ions in the structure of colemanite into solution was investigated at 0.05, 0.10, and 0.15 L/min flow rates. The graph of the solution pass values of Ca^{2+} ions versus time is shown in Figure 9. As seen in Figure 9, the increase in the synthetic flue gas flow rate

increases the Ca^{2+} dissolution rate. As seen in Eq.(4) and Eq.(5), the increase in synthetic flue gas flow rate increases the H_3O^+ ion concentration and this increases the dissolution rate of colemanite. Here, as the flow rate of SFG increases, the instantaneous SO_2 concentration in the solution increases. In this case, reactions 3-5 shift to the right and the formation rate of H_3O^+ ions increases. This increases the speed of reactions 6-8.

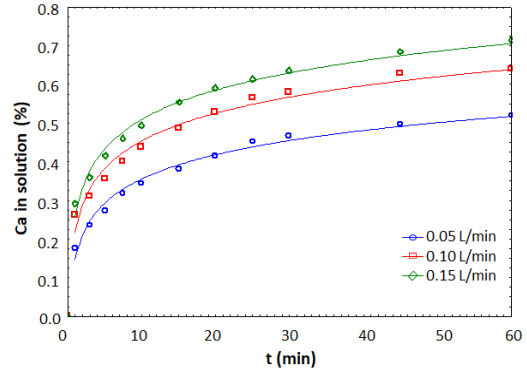


Figure 9. Effect of synthetic flue gas flow rate on Ca^{2+} released during the dissolution of colemanite in SFG saturated solution.

3.3 Kinetic Analysis

Chemical kinetics is a field that enables the derivation of mathematical models describing the rates and mechanisms of the reactions, the direction in which the reaction takes place, and the effects of chemical reactions on the rate and chemical reactions. The chemical reaction can occur in a single phase (homogeneous reaction) or multiple phases (heterogeneous reaction). The dissolution kinetics of Ca^{2+} in solutions saturated with SO_2 in the synthetic flue gas content of colemanite ore were analyzed according to homogeneous and heterogeneous models. The reaction rate equations were tried by the rate control mechanisms and the regression (r^2) values were obtained as in Table 3.

The reaction model with the highest r^2 resistance is considered the step controlling the rate. It was determined that the "Avrami" model was the most suitable model and a kinetic model was derived that represents the process in line with the effects of the parameters. This result is also consistent with the observation of calcium sulfite crystals on colemanite particles.

The reaction rate expression of the Avrami model is seen in Eq.(11).

$$kt^m = -\ln(1-x) \quad (11)$$

If the logarithm of Eq.(11) is taken;

$$\ln k + m \ln t = \ln[-\ln(1-x)] \quad (12)$$

Eq.(12) is obtained.

Table 3. Reaction rate equations were tried in modeling and r^2 values found

Equations	Speed Control Models	r^2
$kt^m = -\ln(1-X)$	Avrami	0.931
$kt = 1-3(1-X)^{2/3} + 2(1-X)$	Ash film diffusion control for fixed-size spheres	0.850
$kt = -\ln(1-X)$	1. Pseudo homogenous reaction model	0.528
$kt = X / 1-X$	2. Pseudo homogenous reaction model	0.912
$kt = X^2$	Ash film diffusion control for fixed-size flat plate	0.724
$kt = X + (1-X)\ln(1-X)$	Ash film diffusion control for fixed-size cylinder	0.820

The graphs of $\ln t$ versus $\ln[-\ln(1-x)]$ for different temperature values are given in Figure 10. The $\ln k$ was determined from the value at which each temperature line intercepts the ordinate.

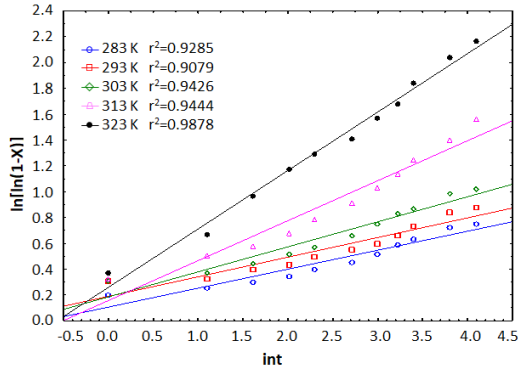


Figure 10. Variation of $\ln[-\ln(1-X)]$ versus $\ln t$ for different reaction temperatures.

The graph shows that each temperature line forms a curve. The reaction rate constant k , which is dependent on the temperature, is found from the slope of temperature lines in Figure 10 and is used to identify the relation between k and T in the Arrhenius equation [29,30].

$$k = Ae^{-E/RT} \quad (13)$$

Eq.(14) is obtained by taking the natural logarithm of Eq.(13).

$$\ln k = \ln A - E/RT \quad (14)$$

The Arrhenius graph in Figure 11 is obtained by graphing $\ln k$ versus $1/T(K)$ for each temperature value. The activation energy (E) was calculated as 26.83 $\text{kJ}\cdot\text{mol}^{-1}$ and the Arrhenius constant (A) was calculated as $8.9 \cdot 10^3$ from the slope and y-intercept of the Arrhenius graph, respectively. The determination of the activation energy of the process as 26.83 $\text{kJ}\cdot\text{mol}^{-1}$, that is, not above 40 kJ/mol , confirms that the dissolution rate of the process is controlled by diffusion from the Avrami model [31]. Similar results were obtained by dissolving colemanite, nitric acid, ammonium hydrogen sulfate, oxalic acid, and ulexite in perchloric acid and

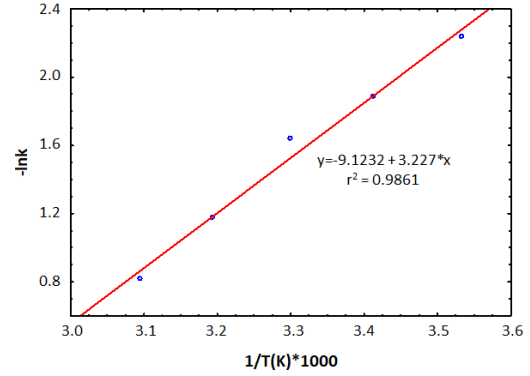


Figure 11. Arrhenius graph of the dissolution reaction of colemanite.

CO_2 solutions [16,32-35].

$$k = A(KS)^a(D)^b(C)^c(GD)^d e^{-E/RT} \quad (15)$$

Eq.(16) is obtained if the open form of the rate constant (k) in the Avrami model is written in Eq.(15).

$$\ln(1 - X_{Ca}^{2+}) = A(KS)^a(D)^b(C)^c(GD)^d e^{-E/RT} t^m \quad (16)$$

The a, b, c, d, m exponential constants in Eq.(16) were calculated using the Statistica 10 package program with multiple regression method, and the Arrhenius constant and the activation energy were calculated using the Arrhenius graph. The obtained data are written in the appropriate places in Eq.(16), and the mathematical version of the Avrami model is obtained in Eq.(17).

$$\ln(1 - X_{Ca}^{2+}) = 8.9 \cdot 10^3 (KS)^{-0.675} (D)^{-0.196} (C)^{0.279} (GD)^{0.435} e^{-26.83/RT} t^{0.362} \quad (17)$$

The theoretical dissolution percentage values of Ca^{2+} in Figure 12 were calculated using Eq.(17) in the Statistica 10 package program, and the experimental dissolution percentage values were calculated using the Avrami model equation. Sorting the theoretical percent dissolution and experimental dissolution percentage values on the same diagonal in the graph shows that the experimental and theoretical transformation results of the model chosen for this process are in harmony with each other.

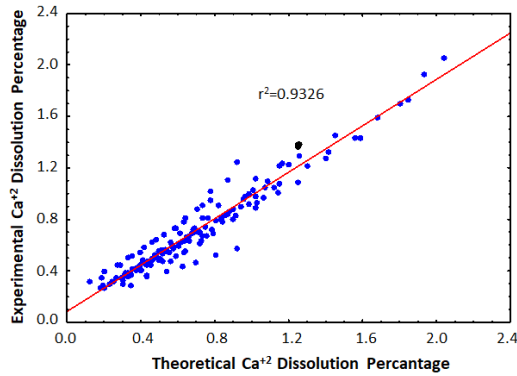


Figure 12. Harmony of experimental and theoretical conversion values.

4. Conclusion

In this study, an alternate reactant was proposed for the production of boric acid, and the kinetics of Ca^{2+} were studied in the dissolution of colemanite in a propionic acid solution saturated with synthetic flue gas in an atmospheric pressure environment. This study has shown that the kinetic model of the dissolution process of colemanite mineral in propionic acid solutions saturated with synthetic flue gas can be expressed by the Avrami model due to the crystallization of the product and by-products on the mineral surface. It was also determined that the precipitation of $\text{CaSO}_3 \cdot 0.5\text{H}_2\text{O}$, CaCO_3 , and $\text{CaSO}_4 \cdot 2\text{H}_2\text{O}$ on the mineral surface made it difficult for the diffusion of H_3O^+ to the unreacted mineral surface. Following results were obtained;

- As the reaction temperature, acid concentration, and synthetic flue gas flow rate increase, the amount of Ca^{2+} passing into the solution and its rate of passing increase. The same results were obtained in studies on the effect of temperature increase and increase in acid concentration on the dissolution of colemanite.
- As the solid-liquid ratio and grain size increase, the Ca^{2+} ions that pass into the solution decrease.
- Weakly acidic propionic acid and synthetic flue gas containing low SO_2 can dissolve colemanite ore for boric acid production. It is suitable as a new solvent reactant for a boric acid production process which the generation of environmentally harmful by-products (borogypsum) is minimal.
- Homogeneous and heterogeneous models were tried on the experimental results to determine the dissolution kinetic model of Ca^{2+} that passes into solution in an aqueous medium. It has been determined that the process fits the Avrami model [$\ln(1-X) = kt^m$]. The activation energy was found to be $26.83 \text{ kJ} \cdot \text{mol}^{-1}$.
- A mathematical model based on the specified parameters was derived.

$$-\ln(1-X_{\text{Ca}^{2+}}) = 8.9 \cdot 10^3 (\text{KS})^{-0.675} (\text{D})^{-0.196} (\text{C})^{0.279} (\text{GD})^{0.435} e^{-26.83/\text{RT}} t^{0.362}$$

Symbols

A	: Frequency factor
a, b, c, d, m	: Model constants
C	: Propionic acid concentration (M)
D	: Average particle size (μm)
E	: Activation energy
GD	: Synthetic flue gas flow rate (mL/min)
k	: Reaction rate constant
L	: Liquid amount (mL)
PA	: Propionic acid
R	: Ideal gas constant [$8.314 \text{ kJ} \cdot (\text{kmol} \cdot \text{K})^{-1}$]
r	: Regression coefficient
s	: Solid amount (g)
SFG	: Synthetic flue gas
T	: Temperature (K)
t	: Time (min)
X	: Conversion fraction

Acknowledgement

This study was conducted in the laboratories of Çankırı Karatekin University. The author thanks Prof. Dr. M. Muhtar Kocakerim for support and helpful discussion.

References

- [1]. Doğan, H.T., Yartaşı, A., (2009). Kinetic investigation of reaction between ulexite ore and phosphoric acid. *Hydrometallurgy*, 96(4),294-299. <https://doi.org/10.1016/j.hydromet.2008.11.006>.
- [2]. Eti Maden İşletmeleri, Strateji Geliştirme Dairesi. (2021). Bor Sektör Raporu. https://www.etimaden.gov.tr/storage/2021/Bor_Sektor_Raporu_2020.pdf.
- [3]. İçelli, O., Erzeneoğlu, S., Boncuğuoğlu, R., (2003). Measurement of X-Ray transmission factors of some boron compounds. *Radiation Measurements*, 37(6), 613-616. [https://doi.org/10.1016/S1350-4487\(03\)00049-0](https://doi.org/10.1016/S1350-4487(03)00049-0).
- [4]. Garrett, D.E. (1998). Borates: handbook of deposits, processing, properties, and use. Elsevier. <https://doi.org/10.1016/B978-0-12-276060-0.X5000-1>.
- [5]. Şimşek, H.M., Guliyev, R., Beşe, A.V., İçen, H., (2017). Investigation of the solubility of borogypsum diammonium in hydrogen phosphate solutions. *Journal of Boron*, 2(2):82-86.
- [6]. Sert., H, Yıldırım. H., Toscalı, D., (2012). An investigation on the production of sodium metaborate dihydrate from ulexite by using trona and lime. *International Journal of Hydrogen Energy*, 37(7), 5833-5839. <https://doi.org/10.1016/j.ijhydene.2012.01.012>.
- [7]. Karagöz. Ö., Kuşlu. S., (2021). Synthesis of pure potassium pentaborate (KB5) from potassium dihydrogen phosphate (KH_2PO_4) and colemanite. *Chemical Papers*, 75, 5963-5969. <https://doi.org/10.1007/s11696-021-01771-z>.
- [8]. Şimşek. H.M., Yeşilyurt, M., (2021). Investigation of the kinetic mechanism of colemanite in Sodium Bisulfate

- solution. *Journal of Boron*, 6(4), 395-401. <https://doi.org/10.30728/boron.959361>.
- [9]. Arasu, A.V., Sornakumar, T., (2007). Design, manufacture and testing of fiberglass reinforced parabola trough for parabolic trough solar collectors. *Solar Energy*, 81(10),1273-1279. <https://doi.org/10.1016/j.solener.2007.01.005>.
- [10]. Künkül, A., Yapici, S., Kocakerim, M.M., Copur, M., (1997). Dissolution kinetics of ulexite in ammonia solutions saturated with CO₂. *Hydrometallurgy*, 44(1-2),135-145. [https://doi.org/10.1016/S0304-386X\(96\)00037-0](https://doi.org/10.1016/S0304-386X(96)00037-0).
- [11]. Tombal, T., Özkan, Ş., Kurşun Ünver İ, Osmanlioğlu, A., (2016). Properties, production, uses of boron compounds and their importance in nuclear reactor technology. *Journal of Boron*, 1(2),86-95. <https://dergipark.org.tr/en/pub/boron/issue/24508/259751>.
- [12]. Çalimli, M.H., Mehmet, T., Kocakerim, M.M., (2020). Investigation dissolution behaviours and kinetics parameters of ulexite in boric acid solution. *International Journal of Chemistry and Technology*, 4(2),121-129. <https://doi.org/10.32571/ijct.734917>.
- [13]. Balasubramanian, R., Lakshmi Narasimhan, T., Viswanathan, R., Nalini, S., (2008). Investigation of the vaporization of boric acid by transpiration thermogravimetry and Knudsen effusion mass spectrometry. *The Journal of Physical Chemistry B*, 112(44),13873-13884. <https://doi.org/10.1021/jp8058883>.
- [14]. Mumcu Şimşek, H., Guliyev R., A. (2022). Taguchi Optimization Study about the Dissolution of Colemanite in Ammonium Bisulfate (NH₄HSO₄) Solution. *Iran J Chem Chem Eng Research Article Vol*, 41(8). <https://doi.org/10.30492/ijcce.2021.530973.4757>.
- [15]. Kurtbaş, A., Kocakerim, M.M., Küçük, Ö., Yartaşı, A. (2006). Dissolution of colemanite in aqueous solutions saturated with both sulfur dioxide (SO₂) gas and boric acid. *Industrial & Engineering Chemistry Research*, 45(6),1857-1862. <http://dx.doi.org/10.1021/ie050050i>.
- [16]. Guliyev, R., Kuşlu, S., Çalban, T., Çolak, S. (2012). Leaching kinetics of colemanite in ammonium hydrogen sulphate solutions. *Journal of Industrial and Engineering Chemistry*, 18(4),1202-1207. <http://dx.doi.org/10.1016/j.jiec.2011.11.082>.
- [17]. Kizilca, M., Copur, M., (2015). Kinetic investigation of reaction between colemanite ore and methanol. *Chemical Engineering Communications*, 202(11),1528-1534. <http://dx.doi.org/10.1080/00986445.2014.956739>.
- [18]. Helvacı, C. (2017). Borate deposits: An overview and future forecast with regard to mineral deposits. *Journal of Boron*, 2(2), 59-70. <https://dergipark.org.tr/en/pub/boron/issue/31236/302668>.
- [19]. Sis. H., Bentli, I., Demirkiran, N., Ekmekyapar, A. (2019). Investigating dissolution of colemanite in sulfuric acid solutions by particle size measurements. *Separation Science and Technology*, 54(8),1353-1362. <http://dx.doi.org/10.1080/01496395.2018.1532961>.
- [20]. Abi, C.E. (2014). Effect of borogypsum on brick properties. *Construction and Building Materials*, 59,195-203. <http://dx.doi.org/10.1016/j.conbuildmat.2014.02.012>.
- [21]. Bulutcu, F., Dogrul, A., Güç, M.O. (2002). The involvement of nitric oxide in the analgesic effects of ketamine. *Life Sciences*, 71(7),841-853. [https://doi.org/10.1016/s0024-3205\(02\)01765-4](https://doi.org/10.1016/s0024-3205(02)01765-4).
- [22]. Tunç, M., Kocakerim, M.M., Küçük, Ö., Aluz, M. (2007). Dissolution of colemanite in (NH₄)₂SO₄ solutions. *Korean Journal of Chemical Engineering*, 24, 55-59. <http://dx.doi.org/10.1007/s11814-007-5009-0>.
- [23]. Bulutcu, A., Ertekin, C., Celikoyan, M.K. (2008). Impurity control in the production of boric acid from colemanite in the presence of propionic acid. *Chemical Engineering and Processing: Process Intensification*, 47(12),2270-2274. <http://dx.doi.org/10.1016/j.cep.2007.12.012>.
- [24]. Phechkrajang, C.M., Yooyong, S. (2017). Fast and simple method for semiquantitative determination of calcium propionate in bread samples. *Journal of Food and Drug Analysis*, 25(2),254-259. <https://doi.org/10.1016/j.jfda.2016.03.013>.
- [25]. Tunç, M., Kocakerim, M.M., Küçük, Ö., Aluz, M. (2007). Dissolution of colemanite in (NH₄)₂SO₄ solutions. *Korean Journal of Chemical Engineering*, 24,55-59. <http://dx.doi.org/10.1007/s11814-007-5009-0>.
- [26]. Şimşek, H.M., Guliyev, R., Beşe, A.V. (2018). Dissolution kinetics of borogypsum in di-ammonium hydrogen phosphate solutions. *International Journal of Hydrogen Energy*, 43(44),20262-20270. <http://dx.doi.org/10.1016/j.ijhydene.2018.07.089>.
- [27]. Cetin, E., Eroğlu, İ., Özkar, S. (2001). Kinetics of gypsum formation and growth during the dissolution of colemanite in sulfuric acid. *Journal of Crystal Growth*, 231(4),559-567. [https://doi.org/10.1016/S0022-0248\(01\)01525-1](https://doi.org/10.1016/S0022-0248(01)01525-1).
- [28]. Okur, H., Tekin, T., Ozer, A.K., Bayramoglu, M. (2002). Effect of ultrasound on the dissolution of colemanite in H₂SO₄. *Hydrometallurgy*, 67(1-3), 79-86. [http://dx.doi.org/10.1016/S0304-386X\(02\)00137-8](http://dx.doi.org/10.1016/S0304-386X(02)00137-8).
- [29]. Abanades, S., Kimura, H., Otsuka, H. (2015). Kinetic investigation of carbon-catalyzed methane decomposition in a thermogravimetric solar reactor. *International Journal of Hydrogen Energy*. 40(34),10744-10755. <https://doi.org/10.1016/j.ijhydene.2015.07.023>.
- [30]. Naktiyok, J., Bayrakçeken, H., Özer, A.K., Gülaboğlu, M.Ş. (2013). Kinetics of thermal decomposition of phospholipids obtained from phosphate rock. *Fuel Processing Technology*, 116,158-164. <http://dx.doi.org/10.1016/j.fuproc.2013.05.007>.
- [31]. Levenspiel, O. (1998). Chemical reaction engineering: *John Wiley & Sons*. ISBN:978-0-471-25424-9.
- [32]. Alkan, M., Doğan, M. (2004). Dissolution kinetics of colemanite in oxalic acid solutions. *Chemical Engineering and Processing: Process Intensification*, 43(7),867-872. [https://doi.org/10.1016/S0255-2701\(03\)00108-9](https://doi.org/10.1016/S0255-2701(03)00108-9).
- [33]. Bayca, S.U., Kocan, F., Abali, Y. (2014). Dissolution of colemanite process waste in oxalic acid solutions. *Environmental Progress & Sustainable Energy*, 33(4),1111-1116. <https://doi.org/10.1002/ep.11889>.

- [34]. Demirkıran, N., Künkül, A. (2007). Dissolution kinetics of ulexite in perchloric acid solutions. *International Journal of Mineral Processing*, 83(1-2),76-80. <http://dx.doi.org/10.1016/j.minpro.2007.04.007>.
- [35]. Elçiçek, H., Kocakerim, M.M. (2018). Leaching kinetics of ulexite ore in aqueous medium at different CO₂ partial pressures. *Brazilian Journal of Chemical Engineering*, 35,111-122. <https://doi.org/10.1590/0104-6632.20180351s20160084>.

Appendices

Appendix-A1

Table A1. Kinetic study experiment plan.

Experiment No	Reaction Temperature (K)	Solid/Fluid Ratio (g/L)	Particle Size (µm)	Acid Concentration (M)	SFG Flow Rate (L/min)
1	183	40	250-400	0.675	0.10
2	293	40	250-400	0.675	0.10
3	303	404	250-400	0.675	0.10
4	313	40	250-400	0.675	0.10
5	323	20	250-400	0.675	0.10
6	303	60	250-400	0.675	0.10
7	303	80	250-400	0.675	0.10
8	303	40	250-400	0.675	0.10
9	303	40	250-400	0.675	0.10
10	303	40	100-150	0.675	0.10
11	303	40	150-250	0.675	0.10
12	303	40	400-600	0	0.10
13	303	40	250-400	0.3378	0.10
14	303	40	250-400	1.335	0.10
15	303	40	250-400	0.675	0.05
16	303	40	250-400	0.675	0.15